

RESEARCH

Open Access



The damage and remineralization strategies of dental hard tissues following radiotherapy

Lin Yao^{1†}, Yanyao Li^{1†}, Di Fu¹, Ye Wang¹, Chengge Hua², Ling Zou³ and Li Jiang^{2*}

Abstract

Objectives This study pursued two main purposes. The first aim was to expound on the microscopic factors of radiation-related caries (RRC). Further, it aimed to compare the remineralization effect of different remineralizing agents on demineralized teeth after radiotherapy.

Methods The enamel and dentin samples of bovine teeth were irradiated with different doses of radiation. After analysis of scanning electron microscope (SEM), X-Ray diffraction (XRD), and energy dispersive spectrometer (EDS), the samples irradiated with 50 Gy radiation were selected and divided into the demineralization group, the double distilled water (DDW) group, the Sodium fluoride (NaF) group, the Casein phosphopeptide-amorphous calcium phosphate (CPP-ACP) group, the NaF + CPP-ACP group, and the Titanium tetrafluoride (TiF₄) group. After demineralization, remineralizing agents treatment, and remineralization, the samples were evaluated using SEM, atomic force microscope (AFM), EDS, and transverse microradiography (TMR).

Results A radiation dose of 30 Gy was sufficient to cause damage to the dentinal tubules, but 70 Gy radiation had little effect on the microstructure of enamel. Additionally, the NaF + CPP-ACP group and the TiF₄ group significantly promoted deposit formation, decreased surface roughness, and reduced mineral loss and lesion depth of demineralized enamel and dentin samples after radiation.

Conclusions Radiation causes more significant damage to dentin compared to enamel. NaF + CPP-ACP and TiF₄ had a promising ability to promote remineralization of irradiated dental hard tissues.

Advances in knowledge This in vitro study contributes to determining a safer radiation dose range for teeth and identifying the most effective remineralization approach for RRC.

Keywords Radiotherapy, Radiation-related caries, Dental hard tissue remineralization, Titanium tetrafluoride, Casein phosphopeptide-amorphous calcium phosphate

[†]Lin Yao and Yanyao Li contributed equally to this work.

*Correspondence:

Li Jiang
echojiang999@sina.com

¹State Key Laboratory of Oral Diseases, West China Hospital of Stomatology, National Clinical Research Center for Oral Diseases, Sichuan University, Chengdu 610041, China

²State Key Laboratory of Oral Diseases, Department of General Dentistry, West China Hospital of Stomatology, National Clinical Research Center for Oral Diseases, Sichuan University, Chengdu 610041, China

³State Key Laboratory of Oral Diseases, Department of Endodontics, West China Hospital of Stomatology, National Clinical Research Center for Oral Diseases, Sichuan University, Chengdu 610041, China



Introduction

Head and neck cancer (HNC) standing as the seventh most common malignancy in the world [1, 2], mainly occurs at sites including the oral cavity, nasopharynx, oropharynx, hypopharynx, larynx, and trachea [3]. Radiotherapy is of vital importance in HNC management [4]. Despite enhancing patient survival rates, it often results in severe tissue damage [5], and the early or late adverse events stemming from radiotherapy of HNC are difficult to control. Radiation may have implications for various components within the oral cavity, including the oral mucosa, salivary glands, bones, masticatory muscles, and dentition of afflicted individuals. Early-stage radiotherapy often manifests with symptoms such as taste loss and diminished salivary gland function, directly or indirectly contributing to radiation-related caries (RRC) [6].

RRC is an invasive condition that occurs in HNC patients undergoing radiotherapy. One of the typical features of RRC is that lesions start on the cervical areas of labial surfaces, progress around the tooth cervical areas [6], and form a “cervical ring” [7]. Radiation can cause changes in the chemical composition, especially the organic component, of dental hard tissues, thereby altering their biomechanical properties. Moreover, due to the higher content of organic components in the enamel-dentinal junction (EDJ) and dentin, the impact of radiation on EDJ and dentin is relatively greater compared to enamel [8, 9]. Radiotherapy may also have an impact on the polymerization and bonding of resins, making subsequent dental restorations challenging [8]. If not diagnosed and treated in time, RRC will lead to tooth fractures [10], or even tooth loss [11]. At present, there is no widely acknowledged clinical treatment for effectively repairing RRC with a high success rate. Hence, the prevention and management of RRC are necessary to enhance the quality of life for HNC patients following radiotherapy [12, 13].

To prevent RRC, we should first understand the etiology, and the damage of enamel and dentin caused by radiation is an internal factor. Kudkuli et al. argued that radiotherapy caused substantial alterations in both the inorganic and organic functional groups on the enamel surface [14]. Radiation doses exceeding 40 Gy could reduce the microhardness of enamel and dentin, affecting their bonding capacity [15]. Conversely, Gonçalves et al. suggested that radiation did not directly affect the inorganic structure of human teeth or alter the overall microhardness of enamel. The observed changes in enamel's physical properties after radiotherapy are attributed to alterations in the organic matrix within the enamel [16]. Lu et al. found that the protein-to-mineral ratio in enamel increased following cumulative radiation, while the ratio in dentin decreased [17]. Although a lot of studies showed the effect of gamma radiation on teeth, their

views were quite different. Thus, the effect of radiation on dental hard tissues needs further study.

Demineralization and remineralization of dental hard tissues in the oral cavity are always alternating. However, under pathological conditions, demineralization is stronger than remineralization [18], natural remineralization alone is not enough [19]. To manage RRC, promoting tooth remineralization is an effective non-invasive treatment method. Fluorid-based strategies remain the standard for caries prevention and management [20]. Sodium fluoride (NaF) is a widely used anti-caries agent in clinical practice nowadays. The application of fluoride varnish for three months has been shown to effectively reduce the incidence of RRC [21]. It is reported that the remineralization effect of fluoride is dose-dependent, toothpaste containing 5000 ppm fluoride is more effective for remineralization of root caries lesions than toothpaste containing 1000 to 1500 ppm fluoride [22]. Therefore, a supplement or alternative medicine is needed to control the dose of fluoride and enhance fluoride effects, especially in high-caries-risk individuals and groups of people [19].

Casein phosphopeptide-amorphous calcium phosphate (CPP-ACP) is a novel nano-scale biological anti-caries agent derived from milk protein, which is probably the most studied non-fluoride remineralizing agent [19]. Some reviews suggested that the quantity and quality of clinical trial evidence were insufficient to demonstrate the long-term effectiveness of CPP-ACP in preventing dental caries in vivo [23, 24]. Recently, Shen et al. demonstrated that the inclusion of 5% CPP-ACP in yogurt can enhance enamel caries remineralization [25], and Sim et al. [60] corroborated that toothpaste enriched with NaF and CPP-ACP can enhance the bioavailability of calcium and phosphorus ions, balance the demineralization/remineralization process, and play a positive role in preventing the formation of cervical caries. Moreover, NaF and CPP-ACP have demonstrated their efficacy in halting the progression of root caries [26]. The potential of titanium tetrafluoride (TiF_4) to prevent tooth demineralization has been investigated since 1997 [27]. After the treatment of demineralized bovine teeth with TiF_4 , the uptake of element F in enamel was higher than that of NaF [28]. A clinical trial employing 4% TiF_4 for the prevention of childhood caries indicated that TiF_4 exhibits comparable effectiveness and acceptability in controlling dental caries when compared to NaF [29]. Furthermore, some research indicated that NaF and TiF_4 can mitigate dental hard tissue demineralization following radiation exposure and decelerate caries progression [30]. Nevertheless, limited research has reported the application of these remineralizing agents in the context of promoting dental hard tissue remineralization post-radiotherapy.

To verify the results of previous experiments on the effect of radiation on teeth, and to select a dose that was consistent with clinical practice and significantly increased the risk of RRC for subsequent experiments, we investigated the impact of different radiotherapy doses on the chemical composition and microstructure of tooth enamel and dentin. Additionally, this study compared the effects of diverse remineralization protocols on demineralized bovine teeth enamel and dentin following radiation exposure by scanning electron microscope (SEM), atomic force microscope (AFM), energy dispersive spectrometer (EDS), and transverse microradiography (TMR), aiming to identify the most effective remineralization approach. The null hypotheses were that different doses of radiation had no difference in their effects on the chemical composition and microstructure of dental hard tissues, and the remineralization effect of TiF_4 and $NaF+CPP-ACP$ on dental hard tissues demineralized after radiotherapy was not different from that of NaF or $CPP-ACP$ used individually.

Materials and methods

The flow of experimental methods is shown in Fig. 1.

Materials

Thymol and polymethyl methacrylate were purchased from Macklin (Shanghai, China). NaF , CPP , ACP , and TiF_4 were provided by Macklin (Shanghai, China). In our experiments, the remineralizing agents we used were prepared by dissolving the reagent powder in double distilled water (DDW) to create solutions of the required concentrations. Specifically, the $CPP-ACP$ solution was prepared by mixing equal volumes of 1% CPP solution and 1% ACP solution.

Sample preparation

The required sample size was determined using G*Power 3.1 software. Based on the findings from Turjanski et al. [31], the sample size per group in the first experiment was 4 (20 samples total) with a probability higher than 80%, a statistically significant difference of at least 15%, and a 0.05 significance level. According to the research of Parisay et al [32], The resulting sample size in our second experiment was 10 per group with an effect size of 0.5, a power of 0.8, and a significance level of 0.05. We prepared 13 samples per group (78 samples total) to compensate for laboratory errors.

Incisors of 5-year-old cows purchased from the local slaughterhouse were used in the study. The bovine permanent incisors were soaked in 0.1% thymol solution (Macklin, Shanghai, China) [28], and then the soft tissues and debris on the surface were removed by surgical instruments and an ultrasonic cleaner (FS20; Fisher Scientific Co., Pittsburgh, USA). Intact bovine teeth were divided into enamel blocks and dentin blocks with uniform size by a slow precision cutting machine (Minitom; Struers, Copenhagen, Denmark) and emery cutting saw blade (EXAKT300; EXAKT, Norderstedt, Germany) under running deionized water. The prepared enamel and dentin blocks were embedded in polymethyl methacrylate (Macklin, Shanghai, China) in a square mold of 1 cm × 1 cm, then the sample blocks were ground and polished with 300, 800, 1200, and 1500-grit waterproof silicon carbide paper (Yu Ying, Foshan, China) in water-cooled carborundum discs (Struers Minitom; Struers, Copenhagen, Denmark), and the surfaces of enamel and dentin were exposed to at least 4×4 mm². Finally, 98 enamel samples and 98 dentin samples were obtained, which were soaked in PBS solution and stored in a refrigerator at 4 °C.

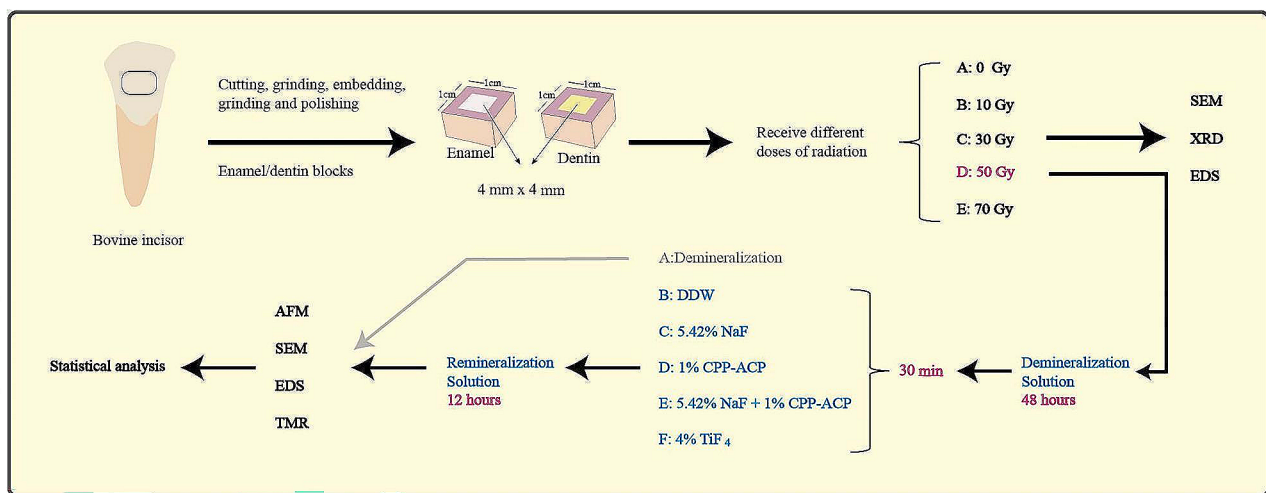


Fig. 1 The flowchart of the experimental procedure

Exploring the impact of different doses of radiation on the microstructure and chemical composition of enamel and dentin

Sample irradiation

Twenty enamel samples and twenty dentin samples were randomly divided into five groups: 0 Gy (Control group), 10 Gy, 30 Gy, 50 Gy, and 70 Gy group ($N=4$). The medical linear accelerator (Synergy; Elekta, Stockholm, Sweden) was used to irradiate the samples, the irradiation distance was 100 cm (from the window surface), the irradiation field was $20 \times 20 \text{ cm}^2$, and the irradiation power was 2.5 Gy/min. We used fractionated radiation, and all samples were within the pre-set radiation field range. To prevent machine overload, samples were irradiated for 2 minutes each time and then cooled for 10 min, followed by the next round of irradiation. Except for the control group, samples of the other four groups received corresponding radiation doses of 10 Gy, 30 Gy, 50 Gy, and 70 Gy, respectively by controlling the irradiation time.

Morphological characterization

Enamel and dentin samples were cut and polished into $4 \times 4 \times 2 \text{ mm}^3$ sample blocks. After ultrasonic cleaning, they were dehydrated by 25%, 50%, 75%, and 95% ethanol solution in turn. Then, these samples were placed in a vacuum gold plating machine and sprayed with gold [33]. Finally, SEM (Apreo 2; Thermo Fisher Scientific, Brno, Czech) was performed to observe the microstructure of enamel and dentin at a magnification of $5000 \times$ and $40,000 \times$, a working distance of $10 \pm 1 \text{ mm}$, and an accelerating voltage of 20 kV.

Element analysis

After treatment with the experimental steps described above for SEM, the appropriate areas in samples were selected in the scanning area of SEM, and the line scanning was carried out by EDS (X-MaxN; Oxford instrument, Oxford, UK) [34]. The measured data were compared and analyzed after a smooth line diagram, and the content and distribution of Ca, P, and C elements in enamel and dentin were detected.

Structural analysis

Through cutting and grinding, the samples with large and uniform windows were selected in each group. XRD (X'pert PRO; Malvern PANalytical, Almelo, Netherlands) measurements were performed, using $\text{CuK}\alpha$ radiation, to scan and record these samples in the range of 2θ (i.e. $10\text{--}60^\circ$ in 0.01° step). The final XRD results were analyzed by HighScorePlus version 5.1 (Malvern PANalytical, Almelo, Netherlands) to detect the crystal structures in enamel and dentin [35].

Exploring the remineralization effect of different remineralizing agents on demineralized dental hard tissues after radiation

After a comprehensive analysis of the results of *experiment 2.2*, we chose a radiation dose of 50 Gy for the next experiment.

Sample irradiation

Seventy-eight enamel samples and seventy-eight dentin samples were irradiated with 50 Gy radiation according to the method above.

Processing of sample blocks

The sample blocks were placed in a demineralizing solution (2.2 mM KH_2PO_4 , 2.2 mM $\text{Ca}(\text{NO}_3)_2$, 5.0 mM NaN_3 , 0.5 ppm NaF, 50 mM acetic acid, pH 4.5) at 37°C for 48 h [37]. The demineralized sample blocks were washed with DDW for 2 min and then dried. Enamel and dentin samples were randomly divided into 6 groups ($N=13$) and treated as follows: (1) demineralization group: no treatment, (2) DDW group: samples treated with DDW for 30 min, (3) NaF (Macklin, Shanghai, China) group: samples treated with 5.42% NaF solution for 30 min, (4) CPP-ACP (Macklin, Shanghai, China) group: samples treated with 1% CPP-ACP solution for 30 min, (5) NaF+CPP-ACP group: samples treated with a mixed solution of 5.42% NaF and 1% CPP-ACP for 30 min, (6) TiF_4 (Macklin, Shanghai, China) group: samples treated with 4% TiF_4 solution for 30 min. The remineralizing agents were brushed onto the sample surface three times with micro brushes (Jaan, Guangzhou, China), with each application repeating after a 10-minute interval. This ensured that the sample surface remained moist for a total of 30 min. The treatment groups (2)-(6) were washed with DDW for 2 min, then placed in remineralizing solution (20 mM HEPES, 0.9 mM KH_2PO_4 , 1.5 mM CaCl_2 , 130 mM KCl, pH 7.0) at 37°C for 12 h [36]. After finishing, the surface was washed with DDW for 2 min and dried for subsequent experiments.

SEM observation

Samples from each group were cut and polished into $4 \times 4 \times 2 \text{ mm}^3$ sample blocks. The following experimental methods were consistent with those in 2.3.2. SEM was operated for scanning and image acquisition.

AFM observation

After demineralization and remineralization, samples from each group were scanned by AFM (SPM9700; Shimadzu, Kyoto, Japan), with a scan area of $5 \times 5 \mu\text{m}^2$ and a scanning frequency of 1 Hz. Shimadzu SPM-9700 software (Shimadzu, Kyoto, Japan) was used to analyze the images, and the surface roughness (Ra) of each sample

was calculated. Finally, statistical analysis was carried out [34].

EDS examination

The following experimental methods were consistent with those in 2.2.3. The changes of Ca, P, C, fluorine (F), and titanium (Ti) elements in the range of 80 μm from the sample surface were analyzed.

TMR examination

Samples were cut into 1 mm-thick slices perpendicular to the window opening surfaces with a slow-cutting machine. All the thin slices were polished to a thickness of 100–120 μm via 1500 grit carbide-polishing papers (Yu Ying, Foshan, China) [37], and the vernier caliper (Mitutoyo, Tokyo, Japan) was used to confirm that the thickness reached the standard. Each slice was then fixed on a TMR imaging slide (Konica Minolta, Tokyo, Japan) and micro-radiographed alongside an aluminum calibration stepwedge with 11 steps for 30 min with a monochrome CuK X-ray source (voltage: 20 kV, current: 20 mA, working distance: 40 cm). Photo plates were developed and fixed according to standard procedures. Images were collected using a transmitted light microscope with a 20 \times objective (Zeiss, Oberkochen, Germany), which was equipped with a CCD camera (Canon, Tokyo, Japan) and connected to a computer (TOSHIBA, Tokyo, Japan). Three non-overlapping areas were selected for each sample, and the mineral loss and lesion depth of the samples

were calculated using TMR Software 2006 (Inspektor Research Systems, Amsterdam, Netherlands) [38].

Statistical analysis

Data were analyzed using SPSS 26.0 (IBM; Armonk, New York, USA). Shapiro-Wilk and Levene tests were used to verify the normal distribution and homogeneity of variance of data, respectively. The roughness data (Ra) followed a normal distribution and met the homogeneity of variance, so ANOVA variance analysis was used to test the results, and LSD analysis was used for pairwise comparisons. However, since the data on the mineral loss and the lesion depth could not simultaneously satisfy the normal distribution and homogeneity of variance, the Kruskal-Wallis H test was used to statistically analyze these data. Finally, the median \pm quartile interval was used to represent the obtained data, and the test level $\alpha=0.05$.

Results

The changes in microstructure and chemical composition of dental hard tissues after different doses of irradiation

The microstructure and chemical composition of enamel after radiation

In this experiment, different doses of radiation did not affect the microstructure of the enamel surface (Fig. 2A). XRD phase analysis of enamel showed that hydroxyapatite crystals, composed of Ca, P, O, and H elements, were the main crystals in enamel at radiation doses of 0 Gy, 10 Gy, and 30 Gy. When radiation doses increased to 50 Gy, apatite crystals were composed of Ca, P, O, and H

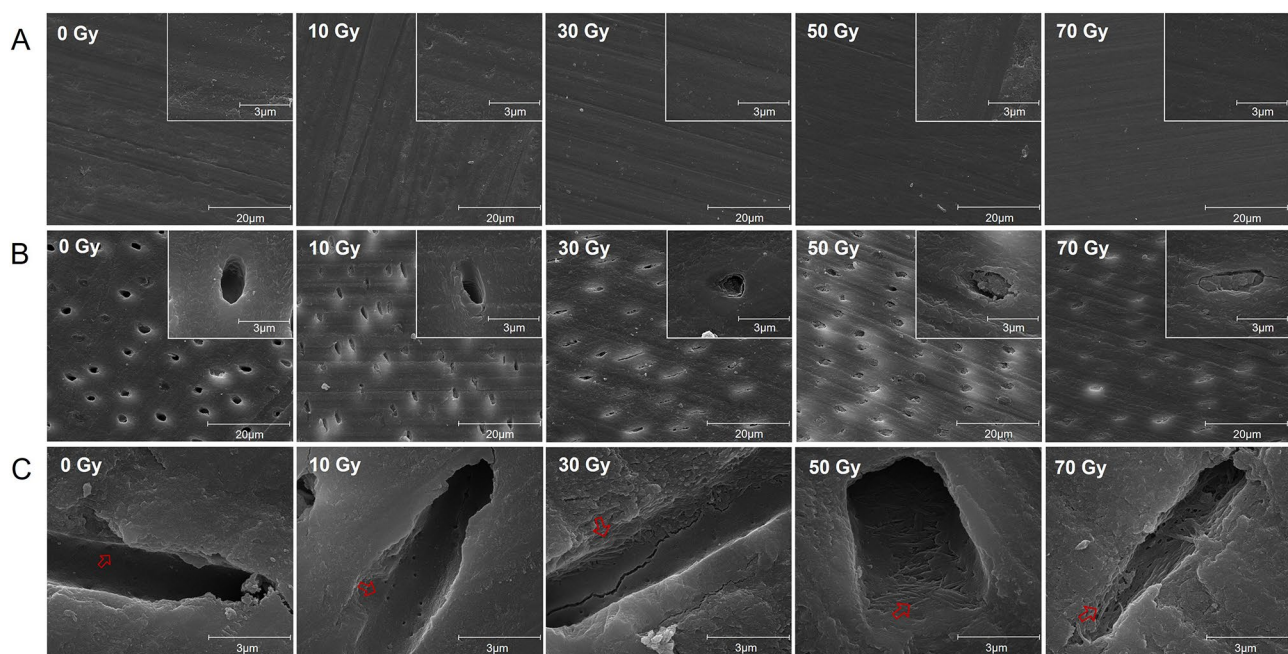


Fig. 2 (A) Representative microstructure of enamel and (B) dentin after different doses of radiation (SEM images, 5000 \times and 40,000 \times). (C) Representative longitudinal section of dentin after different doses of irradiation (SEM images, 40,000 \times). The red arrows indicate typical collagen fiber morphology

elements plus a small amount of Na, Mg, and C elements. When the radiation dose rose to 70 Gy, the content of C element in apatite crystals increased further, and non-apatite crystals, such as potassium calcium and bicarbonate phosphate, appeared at the same time (Fig. 3A).

The microstructure and chemical composition of dentin after radiation

According to the images of SEM, changes were found in the microstructure of dentin. Open dentinal tubules and dense and uniform surfaces in tubules could be seen in groups 0 Gy and 10 Gy, while dentinal tubules gradually collapsed and blocked with the increase of radiation dose (Fig. 2B). From the longitudinal section of dentin tubules, it could be seen that when the radiation dose reached 30 Gy, the inner wall of dentin tubules was no longer smooth and homogeneous, and the dentin collagen fibers became sparse. With the radiation dose increasing to 70 Gy, dentin collagen fibers became disordered from orderly interweaving and obvious fracture could be found (Fig. 2C).

Elemental content of dental hard tissues after radiation

According to the results of EDS, the contents of Ca, P, and C elements in different depths fluctuated slightly,

but there was no obvious difference in the contents of the three elements in enamel (Fig. 3B) and dentin (Fig. 3C) treated by different doses of radiation.

Comparison of the remineralization effects of different remineralizing agents

Changes in surface roughness of dental hard tissues after remineralization

We used AFM to examine the surface roughness of the samples. In the DDW group and the CPP-ACP group, the surface of the enamel showed obvious erosion marks and low smoothness. Dense cluster deposits were formed on the enamel surface of the NaF+CPP-ACP group and the NaF group, making it smooth and uniform. On the surface of the TiF₄ group, spherical deposits with larger diameters were found (Fig. 4A). As for dentin, the surface of the NaF+CPP-ACP group and the NaF group was more uniform than that of the DDW group, and the sediment was denser. The TiF₄ group also had large-diameter spherical sediments (Fig. 4B).

The average surface roughness of each group is shown in Table 1. In enamel samples, there was no significant difference between all remineralized groups, but all remineralized groups had smoother surfaces than the demineralized group (*P*<0.001). In dentin

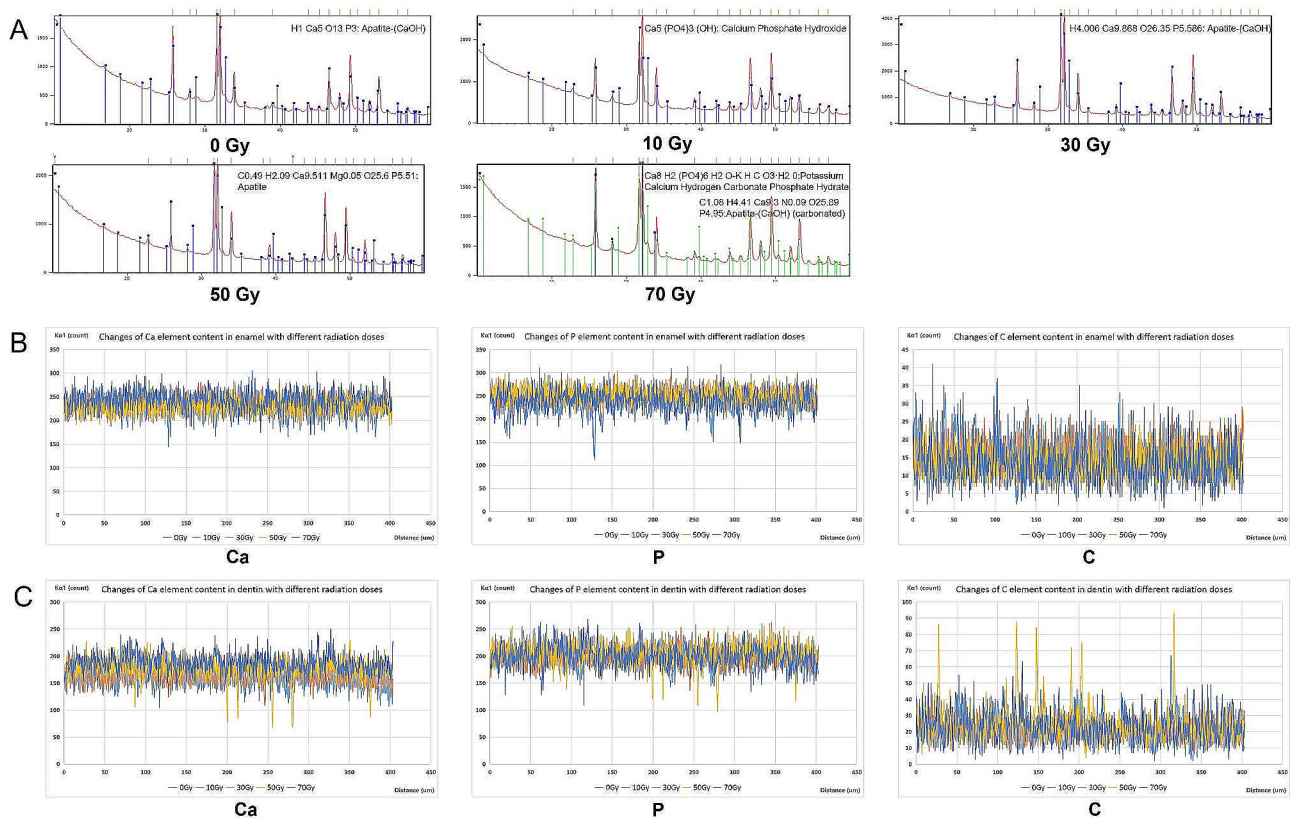


Fig. 3 (A) The XRD phase analysis of enamel after different doses of radiation. (B) The content of Ca, P, and C elements in enamel and (C) dentin at different depths under different radiation doses

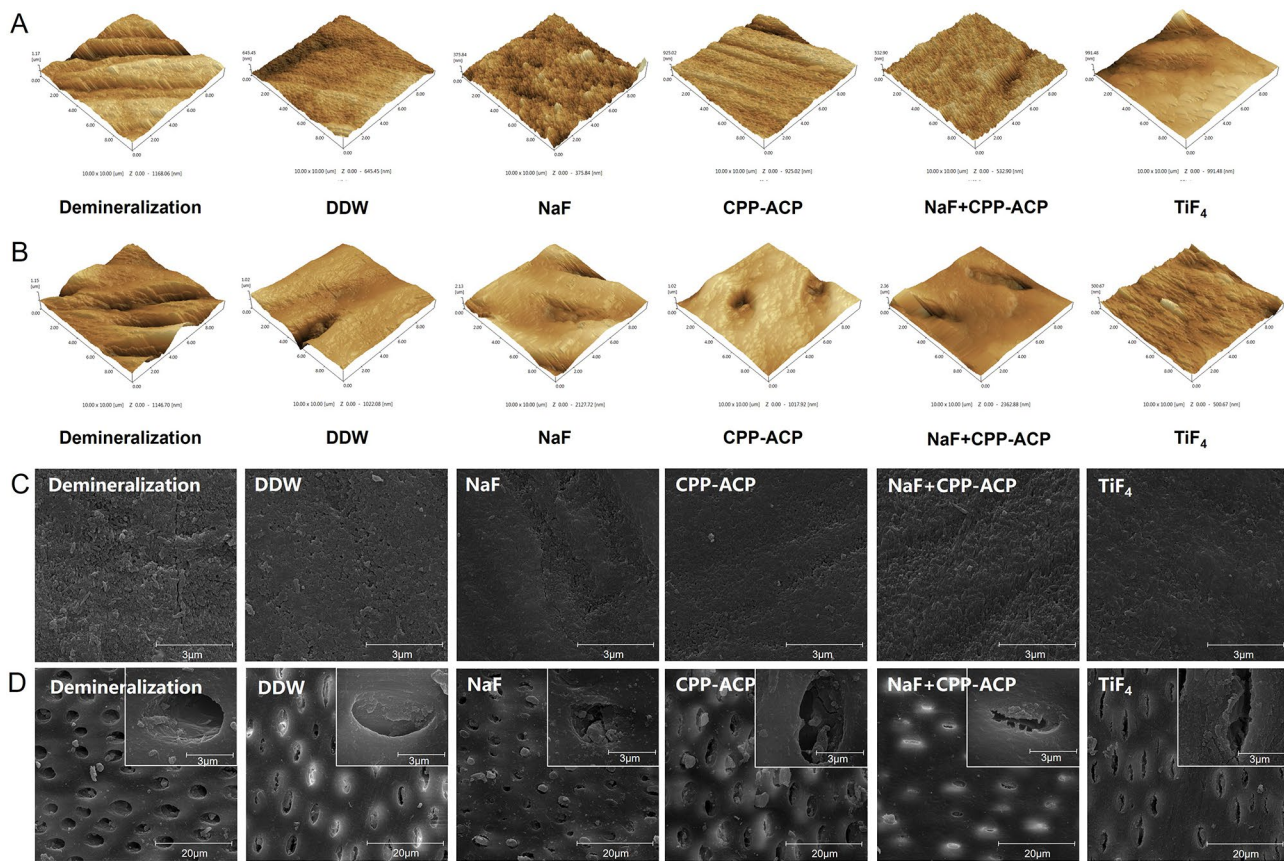


Fig. 4 (A) Representative AFM images of enamel and (B) dentin surfaces in each group. (C) Representative SEM image of enamel in each group (5000 ×). (D) Representative SEM image of dentin in each group (5000 × and 40,000 ×)

Table 1 Quantitative analysis of surface roughness of enamel and dentin in each group

	Enamel		Dentin	
	Roughness (Ra/μm)	P value	Roughness (Ra/μm)	P value
Demineralization	114.12 ± 36.30 ^a	<0.001	145.63 ± 64.30 ^a	<0.05
DDW	63.49 ± 7.53 ^b		123.83 ± 29.05 ^{ab}	
NaF	54.75 ± 10.00 ^b		128.51 ± 40.51 ^{ab}	
CPP-ACP	63.47 ± 9.99 ^b		135.85 ± 26.25 ^a	
NaF + CPP-ACP	56.63 ± 4.28 ^b		99.41 ± 36.49 ^b	
TiF ₄	54.80 ± 12.46 ^b		98.87 ± 21.75 ^b	

All values are presented as means ± SD. The different letters indicate statistically significant differences

samples, the roughness was the lowest in the TiF₄ group (98.87 ± 21.75 nm), followed by the NaF + CPP-ACP group (99.41 ± 36.49 nm). There was a significant difference between the two groups and the demineralization group (*P* < 0.05), but there was no significant difference between other treatment groups and the demineralization group (*P* > 0.05).

The morphology of dental hard tissues after remineralization

The results of SEM showed that compared with the DDW group, the enamel surface of all treatment groups

had denser and more prominent deposits. The enamel surface deposits of the NaF + CPP-ACP group were the most dense and homogeneous, followed by the NaF group, and the CPP-ACP group was between the DDW group and the NaF group. The TiF₄ group formed many large deposits, which were different from the other four groups (Fig. 4C).

For dentin samples, compared with the demineralized group, the dentinal tubules in the DDW group were partially opened, and similar conditions appeared in the dentinal tubules in the CPP-ACP group. The opening degree of dentinal tubules in TiF₄, NaF + CPP-ACP, and NaF groups was limited, and more deposits appeared in most dentinal tubules. At the same time, except for the TiF₄ group, the surface of dentin around the tube was smooth and uniform. Rough and uneven deposits were formed on the surface of dentin around the tube in the TiF₄ group (Fig. 4D).

The changes of contents of Ca, P, F, and Ti elements at different depths after remineralization

EDS analysis of enamel samples (Fig. 5A) and dentin samples (Fig. 5B) showed that TiF₄ had significantly accelerated Ca and P elements deposition. F element

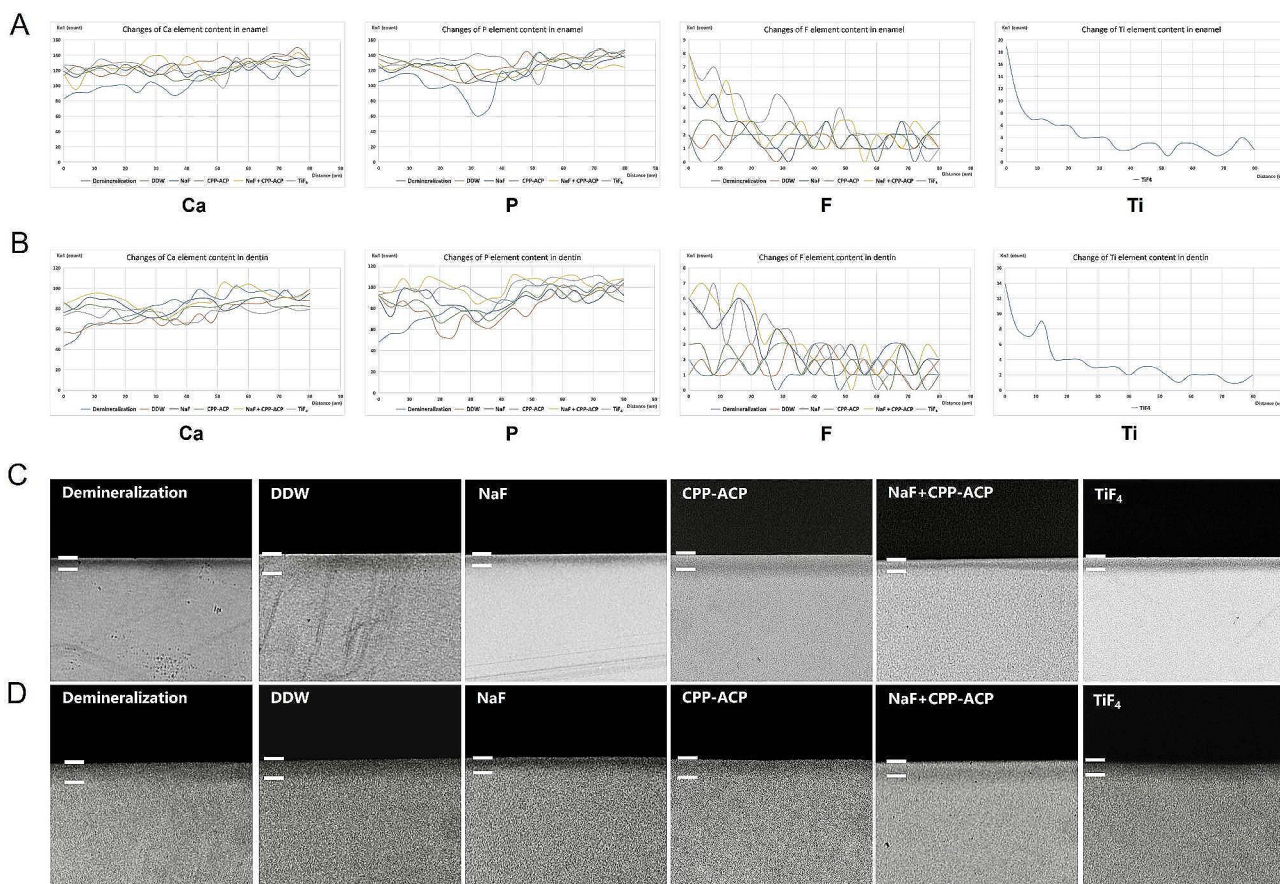


Fig. 5 (A) The changes of Ca, P, F, and Ti elements content in irradiated enamel and (B) dentin at different depths after being treated with different remineralizing agents. (C) TMR images of demineralized enamel and (D) dentin treated with different remineralizing agents

Table 2 Quantitative analysis of mineral loss and lesion depth of demineralized enamel and dentin treated with different remineralizing agents

	Enamel		Dentin	
	Mineral loss (Vol% × μm)	Lesion depth (μm)	Mineral loss (Vol% × μm)	Lesion depth (μm)
Demineralization	1885 ± 1023 ^a	43.65 ± 28.6	900 ± 100 ^a	57.90 ± 5.4
DDW	1025 ± 338 ^a	40.45 ± 26.6	905 ± 340 ^a	53.45 ± 17.9
NaF	780 ± 140 ^b	45.75 ± 16.5	740 ± 300 ^b	53.70 ± 6.7
CPP-ACP	1100 ± 478 ^a	46.25 ± 15.5	900 ± 165 ^a	61.75 ± 26.7
NaF + CPP-ACP	575 ± 215 ^b	37.95 ± 10	645 ± 195 ^b	54.65 ± 12.0
TiF ₄	520 ± 225 ^b	44.95 ± 19.4	580 ± 225 ^b	52.10 ± 11.0

All values are presented as means ± SD. The different letters indicate statistically significant differences

had penetrated up to 20 μm into the enamel lesion in the NaF + CPP-ACP group, while in the NaF group F element penetrated only 5 μm. However, no significant change in the F element was observed in the dentin lesion. In the TiF₄ group, the Ti element had penetrated up to 20 μm into the lesion and 15 μm into the dentin lesion.

Analysis of changes in lesion depth

Representative TMR photos showed that, after TiF₄, NaF, and NaF + CPP-ACP treatment, a remineralization layer with increased density can be observed on the enamel

surface (Fig. 5C), but the remineralization layer in each group of dentin group is not obvious (Fig. 5D).

The results of the quantitative analysis of mineral loss and lesion depth in each group are shown in Table 2. In terms of lesion depth, there was no significant difference between all groups in enamel (P=0.14) and dentin (P=0.593). In enamel samples, mineral loss of the TiF₄ group was 520 ± 225 vol% × μm, which was not significantly different from that of NaF + CPP-ACP and NaF groups (P>0.05), but significantly lower than that of the other three groups (P<0.05). In dentin samples, the

mineral loss in the TiF_4 group was the least (580 ± 225 vol% $\times \mu m$), which had no significant difference with the NaF+CPP-ACP group (645 ± 195 vol% $\times \mu m$) and the NaF group (740 ± 300 vol% $\times \mu m$) but was significantly lower than that in the demineralization group, the DDW group, and the CPP-ACP group.

Discussion

Based on the present results, our null hypotheses were rejected.

The radiation dose ranges from 60 Gy to 70 Gy in the treatment of HNC, which will be partially attenuated after reaching the dental hard tissues [39]. We explored the changes in microstructure and chemical composition of enamel and dentin after different doses of irradiation. In enamel, the XRD findings demonstrated that when the radiation dose reached 50 Gy, there was a gradual replacement of hydroxyapatite, the primary crystal constituent of enamel, by carbonate and other crystals. This observation was consistent with previous research conducted by Hedge et al. [40] and Qing et al. [41], where they reported similar trends. The decrease in crystallinity may have significant implications for the solubility of enamel and dentin, with potential effects on caries susceptibility [42]. As for dentin, when the radiation dosage reached 30 Gy, the dentin tubules began to partially occlude, and the dentin collagen fibers became sparse. When the radiation dose surpassed 50 Gy, nearly all dentin tubules were occluded, and the collagen fibers in the dentin became disordered and fractured. This result was similar to the finding of Walker et al. [43], whose result showed that high-dose radiation would lead to the disappearance of the dentin tubular structure. Taken together, it was found that both enamel and dentin were damaged when the radiation dose exceeded 50 Gy. Therefore, 50 Gy of radiation was selected for subsequent experiments.

Dentin displayed more noticeable changes than enamel in response to different radiation doses in our experiment. This is because there are higher organic content and water composition in dentin compared to enamel and the collagen matrix is highly reactive to radiation [44]. Radiation would change the secondary and tertiary structures of proteins and affect the hydration of collagen fibers, which could lead to the desiccation and fragility of dentin [16]. This explains why RRC is prone to occur in the cervical areas of teeth. Therefore, it is important to maintain the radiation dose below 30 Gy to decrease the risk of RRC in radiotherapy.

Radiation did not induce alterations in the elemental composition and distribution of dental hard tissues in the findings from EDS. To date, there is no available literature addressing radiotherapy causes effects at the atomic level, possibly because the radiation energy employed

in radiotherapy falls significantly below the threshold required to induce atomic-level changes or migrations. Instead, it appears to primarily impact molecular composition and microstructural characteristics.

NaF and CPP-ACP both had been confirmed to have a remineralizing effect in the clinic [21, 25]. NaF not only binds with hydroxyapatite in dental hard tissues to form a more acid-resistant fluorohydroxyapatite [45], but also inhibits the adhesion, proliferation, and metabolism of cariogenic bacteria [46]. The remineralizing mechanism of CPP-ACP involves confining calcium ions, phosphate ions, and fluoride ions to the tooth surface simultaneously and continuously supplying calcium and phosphorus ions to the teeth [47]. In our study, samples were kept in a remineralization solution with rich calcium and phosphorus ions, rendering CPP-ACP ineffective and resulting in no significant difference. However, CPP-ACP can interact with fluoride ions, forming a novel cluster composed of amorphous calcium-fluoride-phosphorus. This composite not only maintains a high concentration of calcium ions, phosphate ions, and fluoride ions on the tooth surface but also prevents the rapid deposition of fluorapatite. It gradually releases the ions required for remineralization to increase the depth of remineralization [48]. This elucidates why the combined use of NaF and CPP-ACP in our study yielded superior remineralization effects compared to NaF alone or CPP-ACP alone group. This is consistent with the study by Llena et al., who indicated that the remineralization efficacy of Casein phosphopeptide-amorphous calcium fluoride phosphate (CPP-ACFP) surpasses that of fluoride varnish [49].

The morphology of dental hard tissues after remineralization was revealed by SEM and AFM images, in which the TiF_4 group and NaF+CPP-ACP group showed better remineralization effects than others. In this research, the enamel surface became rough after radiation exposure and demineralization. Subsequently, after treatment with remineralizing agents and remineralization solution, depositions were observed on the enamel surface. Notably, the enamel surfaces in the NaF group and the NaF+CPP-ACP group displayed dense sedimentation, whereas the TiF_4 group exhibited spherical deposits with larger diameters. Similar trends were observed in dentin samples. According to the findings of Büyükyılmaz et al. [27], the remineralization mechanism of TiF_4 is based on the formation of an acid-resistant layer rich in titanium oxide and hydrated titanium phosphate on the tooth surface. This differs in terms of size and texture from the fluoro-hydroxyapatite induced by NaF or the mineral ions deposition during conventional remineralization [45]. The results of EDS in our experiment corroborated the accumulation of titanium on the surface of dental hard tissues after TiF_4 treatment. Additionally, the results of

AFM indicated that the remineralized sediments produced by the TiF_4 group and NaF+CPP-ACP group were the most abundant and exhibited the lowest surface roughness following remineralization.

In EDS analysis, TiF_4 greatly increased the depth of Ca, P, F, and Ti entering the demineralized enamel and dentin after radiation. In previous research results, compared with NaF varnish, TiF_4 varnish was more effective in inhibiting enamel demineralization and promoting enamel remineralization [26, 46, 50]. This may be related to the low pH value of the TiF_4 solution, which will lead to the dissolution of hydroxyapatite on the enamel surface and the dentin surface, forming a loose and porous structure, enabling calcium, phosphorus, and fluoride ions to enter deeper and obtain better remineralization effect [51]. Although the quantitative analysis of TMR in this study did not reveal a significant difference among the TiF_4 group, the NaF group, and the NaF+CPP-ACP group, when considered in conjunction with TMR and EDS results, it became evident that the penetration depth of F element into enamel and dentin was significantly increased after treatment with TiF_4 and NaF+CPP-ACP compared with NaF.

Based on our experimental results, TiF_4 and NaF+CPP-ACP demonstrated a superior effect in preventing demineralization and promoting remineralization of enamel and dentin compared to other approaches. The protective effect of TiF_4 was associated with the formation of an acid-resistant surface coating and increased fluoride absorption [52], it was perhaps more effective than NaF+CPP-ACP in preventing demineralization. However, the low pH value of TiF_4 also means strict clinical use conditions. When high-concentration TiF_4 is used for remineralization treatment, it is necessary to isolate the other teeth and soft tissues. In addition, we only used bovine teeth for remineralization experiments in vitro, more studies are needed to explore the clinical feasibility of these remineralizing agents in the future.

Conclusions

In this study, the radiation dose within 70 Gy had minimal impact on the microstructure of enamel. However, radiation dose over 50 Gy would lead to the change of crystal phase in enamel. As for dentine, the radiation dose of 30 Gy could affect its microstructure, and the degree of dentin destruction was dose-dependent. In our remineralization experiment, CPP-ACP alone had a poor remineralization effect, but it could promote the remineralization of NaF synergistically. TiF_4 and NaF+CPP-ACP both had a better remineralization effect on demineralized dental hard tissues after radiation than NaF alone. These findings will serve as a theoretical foundation for the prevention and treatment of RRC.

Acknowledgements

Not applicable.

Author contributions

LY Contributed to the conception, and design, and drafted the manuscript. YL Contributed to data acquisition, and interpretation, and performed all statistical analyses. DF and YW Contributed to data acquisition and interpretation. CH, LZ, and LJ Contributed to critically revising the manuscript. All authors gave final approval and agreed to be accountable for all aspects of the work. All authors read and approved the final manuscript.

Funding

This research was supported by the Popular Science Project of Sichuan Science and Technology Department, China (Grant No. 2024JDKP0065).

Data availability

The datasets used and/or analysed during the current study are available from the corresponding author on reasonable request.

Declarations

Ethics approval and consent to participate

This experiment was approved by the Medical Ethics Committee of West China Stomatology Hospital, Sichuan University (WCHSIRB-D-2022-636).

Consent for publication

Not applicable.

Competing interests

The authors declare no competing interests.

Received: 24 March 2024 / Accepted: 3 July 2024

Published online: 16 July 2024

References

- Cohen N, Fedewa S, Chen AY. Epidemiology and demographics of the head and neck cancer population. *ORAL MAXIL SURG CLIN*. 2018;30:381–95.
- Bray F, Ferlay J, Soerjomataram I, Siegel RL, Torre LA, Jemal A. Global cancer statistics 2018: GLOBOCAN estimates of incidence and mortality worldwide for 36 cancers in 185 countries. *Cancer J Clin*. 2018;68:394–424.
- Vigneswaran N, Williams MD. Epidemiologic trends in head and neck cancer and aids in diagnosis. *ORAL MAXIL SURG CLIN*. 2014;26:123–41.
- Moreno AC, Frank SJ, Garden AS, Rosenthal DI, Fuller CD, Gunn GB, et al. Intensity modulated proton therapy (IMPT)—the future of IMRT for head and neck cancer. *ORAL ONCOL*. 2019;88:66–74.
- Mougeot J-LC, Stevens CB, Almon KG, Paster BJ, Lalla RV, Brennan MT, et al. Caries-associated oral microbiome in head and neck cancer radiation patients: a longitudinal study. *J ORAL MICROBIOL*. 2019;11:1586421.
- Kielbassa AM, Hinkelbein W, Hellwig E, Meyer-Lückel H. Radiation-related damage to dentition. *Lancet Oncol*. 2006;7:326–35.
- Velo MM, de AC, Farha ALH, da Silva Santos PS, Shiota A, Sansavino SZ, Souza ATF, et al. Gamma radiation increases the risk of radiation-related root dental caries. *ORAL ONCOL*. 2017;71:184–5.
- Douchy L, Gauthier R, Abouelleil-Sayed H, Colon P, Grosogeat B, Bosco J. The effect of therapeutic radiation on dental enamel and dentin: a systematic review. *Dent Mater*. 2022;38:e181–201.
- Lieshout HFJ, Bots CP. The effect of radiotherapy on dental hard tissue—a systematic review. *Clin Oral Investig*. 2014;18:17–24.
- Palmier NR, Ribeiro ACP, Fônsêca JM, Salvajoli JV, Vargas PA, Lopes MA, et al. Radiation-related caries assessment through the international caries detection and assessment system and the post-radiation dental index. *Oral Surg Oral Med Oral Pathol Oral Radiol*. 2017;124:542–7.
- Chopra A, Monga N, Sharma S, Kumar V, Chawla A, Logani A. Indices for the assessment of radiation-related caries. *J Conserv Dent*. 2022;25:481.
- Duarte VM, Liu YF, Rafizadeh S, Tajima T, Nabili V, Wang MB. Comparison of Dental Health of patients with Head and Neck Cancer receiving IMRT vs Conventional Radiation. *Otolaryngol-head neck surg*. 2014;150:81–6.

13. Frydrych A, Slack-Smith L, Parsons R. Compliance of post-radiation therapy head and neck cancer patients with caries preventive protocols. *AUST DENT J*. 2017;62:192–9.
14. Kudkuli J, Abdulla R, Rekha PD, Sharma SD, Gurjar O. Spectroscopic analyses reveal radiotherapy-induced variations in elemental composition and crystallite properties of human permanent teeth enamel. *J ORAL BIOSCI*. 2019;61:207–14.
15. Muñoz MA, Garín-Correa C, González-Arriagada W, Quintela Davila X, Häberle P, Bedran-Russo A, et al. The adverse effects of radiotherapy on the structure of dental hard tissues and longevity of dental restoration. *INT J RADIAT BIOL*. 2020;96:910–8.
16. Gonçalves LMN, Palma-Dibb RG, Paula-Silva FWG, de Oliveira HF, Nelson-Filho P, da Silva LAB, et al. Radiation therapy alters microhardness and microstructure of enamel and dentin of permanent human teeth. *J Dent*. 2014;42:986–92.
17. Lu H, Zhao Q, Guo J, Zeng B, Yu X, Yu D, et al. Direct radiation-induced effects on dental hard tissue. *Radiat Oncol*. 2019;14:5.
18. Niu L, Zhang W, Pashley DH, Breschi L, Mao J, Chen J, et al. Biomimetic remineralization of dentin. *Dent Mater*. 2014;30. <https://doi.org/10.1016/j.dental.2013.07.013>
19. Philip N. State of the art Enamel Remineralization systems: the Next Frontier in Caries Management. *Caries Res*. 2019;53:284–95.
20. Fontana M. Enhancing fluoride: Clinical Human studies of Alternatives or Boosters for Caries Management. *Caries Res*. 2016;50(Suppl 1):22–37.
21. Dholam KP, Somani PP, Prabhu SD, Ambre SR. Effectiveness of fluoride varnish application as cariostatic and desensitizing agent in irradiated head and neck cancer patients. *Int J Dent*. 2013;2013.
22. Wierichs RJ, Meyer-Lueckel H. Systematic review on noninvasive treatment of root caries lesions. *J Dent Res*. 2015;94:261–71.
23. Azarpazhooh A, Limeback H. Clinical efficacy of casein derivatives: a systematic review of the literature. *J Am Dent Assoc*. 2008;139:915–24. quiz 994–5.
24. Wang Y, Li J, Sun W, Li H, Cannon RD, Mei L. Effect of non-fluoride agents on the prevention of dental caries in primary dentition: a systematic review. *PLoS ONE*. 2017;12:e0182221.
25. Shen P, Fernando JR, Walker GD, Yuan Y, Reynolds C, Reynolds EC. Addition of CPP-ACP to Yogurt inhibits enamel subsurface demineralization. *J Dent*. 2020;103:103506.
26. Sleibi A, Tappuni AR, Baysan A. Reversal of root caries with casein phosphopeptide-amorphous calcium phosphate and fluoride varnish in xerostomia. *CARIES RES*. 2021;55:475–84.
27. Büyükyılmaz T, Ogaard B, Rølla G. The resistance of titanium tetrafluoride-treated human enamel to strong hydrochloric acid. *Eur J Oral Sci*. 1997;105(5 Pt 2):473–7.
28. Comar LP, Souza BM, Al-Ahij LP, Martins J, Grizzo LT, Piasentim IS, et al. Mechanism of action of TiF₄ on dental enamel surface: SEM/EDX, KOH-soluble F, and X-ray diffraction analysis. *CARIES RES*. 2018;51:554–67.
29. de Souza BM, Silva M, de Braga S, Santos AS, Carvalho DMS, de Santos T et al. Acceptability and effect of TiF₄ on dental caries: a randomized controlled clinical trial. *BRAZ ORAL RES*. 2021;35.
30. de Souza BM, Silva MS, Braga AS, Bueno PSK, da Silva Santos PS, Buzalaf MAR, et al. Protective effect of titanium tetrafluoride and silver diamine fluoride on radiation-induced dentin caries in vitro. *Sci Rep*. 2021;11:6083.
31. Turjanski S, Par M, Bergman L, Soče M, Grego T, Klarić Sever E. Influence of Ionizing Radiation on Fluoride-releasing Dental Restorative materials. *Polym (Basel)*. 2023;15:632.
32. Parisay I, Boskabady M, Bagheri H, Babazadeh S, Hoseinzadeh M, Esmaeilzadeh F. Investigating the efficacy of a varnish containing gallic acid on remineralization of enamel lesions: an in vitro study. *BMC Oral Health*. 2024;24:175.
33. Duan M, Liu Y, Guo D, Kan S, Niu Z, Pu X et al. TGF-β2 increases cell-cell communication in chondrocytes via p-Smad3 signalling. *Biochimica et Biophysica Acta (BBA) - molecular Cell Research*. 2022;1869:119175.
34. Jiang N, Su Z, Sun Y, Ren R, Zhou J, Bi R, et al. Spatial heterogeneity directs Energy Dissipation in Condylar Fibrocartilage. *Small*. 2023;19:e2301051.
35. Isaacs MA, Barbero B, Durndell LJ, Hilton AC, Olivi L, Parlett CMA, et al. Tunable silver-functionalized porous frameworks for Antibacterial Applications. *Antibiot (Basel)*. 2018;7:55.
36. Lv X, Yang Y, Han S, Li D, Tu H, Li W, et al. Potential of an amelogenin based peptide in promoting remineralization of initial enamel caries. *Arch Oral Biol*. 2015;60:1482–7.
37. Bakry AS, Abbassy MA. Increasing the efficiency of CPP-ACP to remineralize enamel white spot lesions. *J Dent*. 2018;76:52–7.
38. Fan M, Li M, Yang Y, Weir MD, Liu Y, Zhou X, et al. Dual-functional adhesive containing amorphous calcium phosphate nanoparticles and dimethylamino-hexadecyl methacrylate promoted enamel remineralization in a biofilm-challenged environment. *Dent Mater*. 2022;38:1518–31.
39. Caudell JJ, Torres-Roca JF, Gillies RJ, Enderling H, Kim S, Rishi A, et al. The future of personalised radiotherapy for head and neck cancer. *Lancet Oncol*. 2017;18:e266–73.
40. Hegde MN, Gatti P, Hegde ND. Protection of wear resistance behaviour of enamel against electron beam irradiation. *BDJ open*. 2019;5:11.
41. Qing P, Huang S, Gao S, Qian L, Yu H. Effect of gamma irradiation on the wear behaviour of human tooth enamel. *Sci Rep*. 2015;5:11568.
42. Aoba T. Solubility properties of human tooth mineral and pathogenesis of dental caries. *ORAL DIS*. 2004;10:249–57.
43. Walker MP, Wichman B, Cheng A-L, Coster J, Williams KB. Impact of radiotherapy dose on dentition breakdown in head and neck cancer patients. *PRACT RADIAT ONCOL*. 2011;1:142–8.
44. Maslennikova A, Kochueva M, Ignatieva N, Vitkin A, Zakharkina O, Kamensky V, et al. Effects of gamma irradiation on collagen damage and remodeling. *INT J RADIAT BIOL*. 2015;91:240–7.
45. Buzalaf MAR, Pessan JP, Honório HM, Ten Cate JM. Mechanisms of action of fluoride for caries control. *Monogr Oral Sci*. 2011;22:97–114.
46. Walsh T, Worthington HV, Glenny A-M, Marinho VC, Jeroncio A. Fluoride toothpastes of different concentrations for preventing dental caries. *COCHRANE DB SYST REV*. 2019. <https://doi.org/10.1002/14651858.CD007868.pub3>
47. Morgan MV, Adams GG, Bailey DL, Tsao CE, Fischman SL, Reynolds EC. The anticariogenic effect of sugar-free gum containing CPP-ACP nanocomplexes on approximal caries determined using digital bitewing radiography. *CARIES RES*. 2008;42:171–84.
48. Cross KJ, Huq NL, Stanton DP, Sum M, Reynolds EC. NMR studies of a novel calcium, phosphate and fluoride delivery vehicle-α(S1)-casein(59–79) by stabilized amorphous calcium fluoride phosphate nanocomplexes. *Biomaterials*. 2004;25:5061–9.
49. Llena C, Leyda AM, Forner L. CPP-ACP and CPP-ACFP versus fluoride varnish in remineralisation of early caries lesions. A prospective study. *Eur J Paediatr Dent*. 2015;16:181–6.
50. Comar LP, Wiegand A, Moron BM, Rios D, Buzalaf MAR, Buchalla W, et al. In situ effect of sodium fluoride or titanium tetrafluoride varnish and solution on carious demineralization of enamel. *Eur J Oral Sci*. 2012;120:342–8.
51. Hjortsjö C, Young A, Kiesow A, Cismak A, Berthold L, Petzold M. A descriptive in vitro electron microscopic study of acidic fluoride-treated enamel: potential anti-erosion effects. *Caries Res*. 2016;49:618–25.
52. Salomão PMA, de Oliveira FA, Rodrigues PD, Al-Ahij LP, Gasque KC da, Jeggle S et al. P. The cytotoxic effect of TiF₄ and NaF on fibroblasts is influenced by the experimental model, fluoride concentration and exposure time. *PLoS One*. 2017;12:e0179471.

Publisher's Note

Springer Nature remains neutral with regard to jurisdictional claims in published maps and institutional affiliations.